

## Slow light in coupled-resonator-induced transparency

メタデータ	言語: eng 出版者: 公開日: 2008-02-25 キーワード (Ja): キーワード (En): 作成者: Totsuka, Kouki, Kobayashi, Norihiko, Tomita, Makoto メールアドレス: 所属:
URL	<a href="http://hdl.handle.net/10297/585">http://hdl.handle.net/10297/585</a>

## Slow Light in Coupled-Resonator-Induced Transparency

Kouki Totsuka, Norihiko Kobayashi, and Makoto Tomita

*Department of Physics, Faculty of Science, Shizuoka University, 836 Ohya, Surugaku, Shizuoka, 422-8529 Japan*  
(Received 4 January 2007; published 25 May 2007)

We performed optical pulse propagation experiments in a system in which two ultrahigh- $Q$  silica microspheres of different diameters were coupled in tandem to a fiber taper to yield coupled-resonator-induced transparency. Nearly Gaussian-shaped optical pulses propagated with a large positive delay of 8.5 ns through a transparent frequency window, without significant attenuation, amplification, or pulse deformation, demonstrating classical analogy of the extremely slow light obtained with electromagnetically induced transparency.

DOI: [10.1103/PhysRevLett.98.213904](https://doi.org/10.1103/PhysRevLett.98.213904)

PACS numbers: 42.25.Bs, 42.50.Gy, 42.60.Da

Quantum coherence in atoms has led to several interesting and unexpected outcomes. In electromagnetically induced transparency (EIT), destructive quantum interference introduced by a strong coupling laser cancels the absorption from the ground state to coherent superposing upper states [1]. The observation of nonabsorbing resonance through atomic coherence has led to novel concepts, such as lasing without inversion [2,3]. Since the EIT linewidth can be made extremely narrow, the resultant steep linear dispersion has been used to reduce the velocity of light [4]. This technique has been developed for coherent optical information storage and to freeze light [5,6]. Light storage for times greater than a second has been experimentally demonstrated in solid state system [7].

From the perspective of dispersion engineering or quantum-information storage, dielectric nanostructures appear to be an alternative promising system [8–14]. Since the EIT spectrum results from the interference effect of resonant pathways, similar effects are expected in classical systems. Recently, theoretical analyses and experiments in coupled microsphere resonators have revealed that coherent effects in the system are remarkably similar to those of EIT in atoms [15–17]. Moreover, a new theoretical mechanism for stopping light as a classical analogy to EIT has been proposed using a waveguide side coupled to optical resonators [18,19]. The storage time of the sphere system may be limited by the  $Q$  factors of spheres; this value can be extremely high for microspheres; i.e.,  $Q = 10^{10}$  has been experimentally observed and over  $Q = 10^{21}$  is predicted [20,21]. Here, we performed optical pulse propagation experiments with a system involving coupled-resonator-induced transparency, consisting of two microspheres of different diameters, and demonstrated the classical analogy of extremely slow light in EIT.

Figure 1 is a schematic illustration of the waist region of a coupled resonator consisting of two microspheres ( $S_1$  and  $S_2$ ) and a fiber taper.  $S_1$  and  $S_2$ , with diameters of 39 and 73  $\mu\text{m}$ , respectively, were fabricated from a standard telecommunication optical fiber. The fiber was etched and fused into microsphere form using a  $\text{CO}_2$  laser. A fiber

taper with a typical diameter in the waist region of 0.5  $\mu\text{m}$  was fabricated from the same telecommunication optical fiber [22]. The two microspheres were attached to translation stages controlled with 3-axis piezoactuators. First, we adjusted the position of sphere  $S_1$  relative to the fiber, so that this sphere was coupled to the fiber taper under the undercoupling condition [23]. Then, the position of sphere  $S_2$  was adjusted with respect to  $S_1$  so that a specific whispering gallery mode (WGM) in  $S_2$  was coupled to the resonance mode in  $S_1$ . The resonance frequencies of the two spheres,  $\nu_{S1}$  and  $\nu_{S2}$ , respectively, were adjusted carefully using temperature control. We used the second harmonics of a single-mode ring-cavity  $\text{Nd}^{3+}$ :YAG (yttrium aluminum garnet) laser with a linewidth of 1 kHz at 532 nm. The laser frequency was tuned via thermal control of the cavity length. The mode hop-free scanning range exceeded 10 GHz. Optical pulses were generated using an electro-optic modulator with a repetition rate of 100 kHz. Nearly Gaussian-shaped transform-limited pulses with a pulse width of 51 ns were prepared. The average power of the incident laser was 100 nW. The transmitted pulse profile was observed using a streak camera with a time resolution of 10 ps.

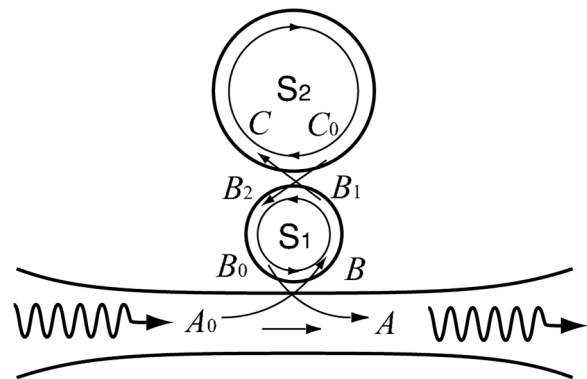


FIG. 1. Schematic illustration of the double microsphere system coupled to a fiber taper.  $S_1$  and  $S_2$  are the first and second spheres, respectively.

To examine the optical characteristics of the double sphere-fiber system, we first examined the transmission spectra. The left column in Fig. 2 shows the transmission spectra as a function of the laser frequency detuning for different gap distances. Figure 2(a) shows the transmission spectrum for the naked first sphere ( $S_1$ ) and fiber system in which the separation gap between spheres was sufficiently large so that the effect of the second sphere ( $S_2$ ) could be neglected. A broad transmission dip appeared when the laser frequency was tuned to resonance frequency  $\nu_{S_1}$  of the WGM in  $S_1$ . The full width at half maximum of the original transmission dip was  $\nu_{S_1} = 150$  MHz, and the minimum transmissivity was  $T_{\min} = 0.08$ . When the gap distance decreased and  $S_2$  was coupled to  $S_1$ ,  $S_2$  modulated the loss and phase of  $S_1$ , and a narrow transparent window appeared at  $\nu_{S_2}$  in the broad absorption band due to  $S_1$ . This peak arose due to destructive interference between the two optical pathways, and we consider this peak as a coupled-resonator-induced transparency: one path passed

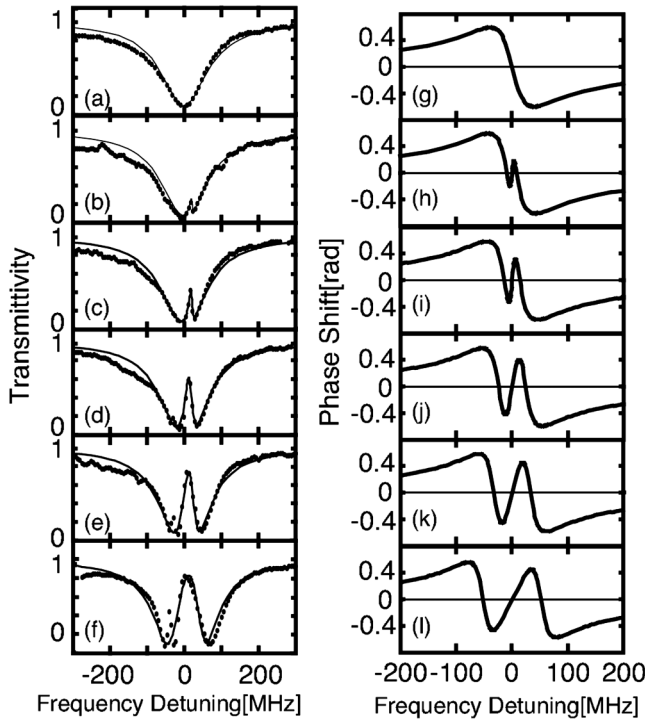


FIG. 2. (a)–(f) The transmission spectra in the double sphere-fiber system as a function of the laser frequency detuning for different separation gap distances. The separation gap decreases from the top to the bottom figures. The solid circles are the experimental observations and the solid curves are the theoretical calculations based on Eq. (2). The frequency origin  $\Delta\nu = 0$  is taken at the resonance frequency of the first sphere,  $\nu_1$ . The parameters used are  $x_1 = 0.999820$  and  $y_1 = 0.999899$ , (b)  $y_2 = 0.99999999$ , (c)  $y_2 = 0.999999974$ , (d)  $y_2 = 0.99999992$ , (e)  $y_2 = 0.999999986$ , and (f)  $y_2 = 0.999999965$ , while  $x_2 = 0.999975 \pm 0.000010$ . (g)–(l) The theoretical calculation of the transmission phase shift as a function of the frequency detuning. The parameters used in (g)–(l) are same as those in (a)–(f), respectively.

$S_2$  and the other path bypassed  $S_2$ . As the gap distance decreased, the induced transmission peak at  $\nu_{S_2}$  increased from  $T_{\text{ind}} = 0.08$  to 0.87, as seen in Fig. 2(a)–2(f), while the frequency width of the transparent window became wider. As the gap distance further decreased, the transmission spectrum split into two separate dips.

We performed pulse propagation experiments and examined the frequency dependence of the propagation delay through the induced transparency window. Figure 3(c) shows the normalized transmitted temporal profile observed at three detuning frequencies denoted as A, B, and C in Fig. 3(a) for a specific gap distance. Time zero was taken at the position of the transmitted pulse peak under the far detuning condition  $\Delta\nu = -240$  MHz. At the center of

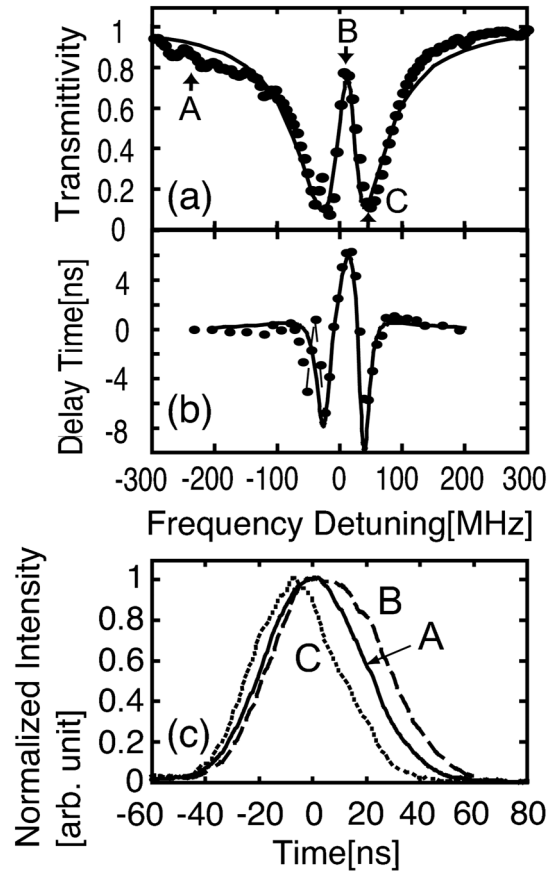


FIG. 3. (a) The transmission spectrum as a function of the laser frequency detuning at a specific gap distance. The solid circles are the experimental observations and the solid curve is the theoretical calculation, where the parameters are  $x_1 = 0.999820$  and  $y_1 = 0.999899$ ,  $x_2 = 0.999975$ ,  $y_2 = 0.999999986$ , and  $\Delta\nu_{12} = 13$  MHz. (b) The pulse propagation delay time through the double sphere-fiber system as a function of the frequency detuning. The solid circles are the experimental observations and the solid curve is the theoretical calculation based on Eq. (2). The parameters used are the same as for (a). (c) Transmitted pulse profiles through the double sphere-fiber system. The solid, dashed, and dotted curves are the pulse profiles at three laser detuning frequencies denoted as A, B, and C in Fig. 3(a), where  $\Delta\nu = -240, 13,$  and  $41$  MHz, respectively.

the induced transparency window, the pulse profile was delayed 6.2 ns, where 78% of the input pulse is transmitted. Therefore, the pulses in this region are propagated through the system with a large positive delay without significant attenuation, amplification, or pulse deformation, demonstrating the classical analogy of extremely slow light in EIT. Figure 3(b) summarizes the propagation delay time as a function of the frequency detuning. The delay time was positive at the center of the transparent window and negative on both sides of the frequency window.

To further investigate slow light in this system, we measured the propagation delay time in the induced transparency window for different gap distances. Figure 4 summarizes our experimental observations of the propagation delay time as a function of coupling parameter  $y_2$  determined from the transmission spectra, as described below. When the gap distance was sufficiently large and the effect of  $S_2$  could be neglected, we observed a negative delay time of  $-6.0$  ns, i.e., fast light relevant to the undercoupling condition of  $S_1$ . As the gap distance decreased, the delay time increased. We observed a maximum positive delay time of  $8.5$  ns at a transmission of  $T_{\text{ind}} = 0.47$ . Figure 4 also plots the width of the induced transparency window  $\Delta\nu_{\text{ind}}$ , which is defined as the frequency difference between the two minima in the transmission spectrum and the transmissivity at the center of the induced transparency  $T_{\text{ind}}$ . When the gap distance decreased further, the propagation delay time again decreased as the frequency width increased.

The stationary input-output characteristics can be analyzed using directional coupling theory [24]. The electrical fields in the fiber at the input and output are denoted  $A_0$  and  $A$ , respectively, and the incoming and outgoing electric fields at the coupling points within the first sphere are denoted  $B$ ,  $B_0$ ,  $B_1$ , and  $B_2$ , and those in the second sphere are  $C$  and  $C_0$ , respectively, as is shown in Fig. 1. Directional coupling theory gives

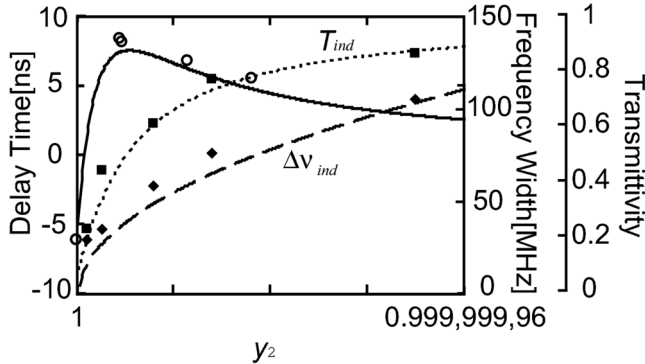


FIG. 4. The open circles, solid diamonds, and solid squares are the experimentally observed propagation delay time (left scale), frequency width of the induced transparency window  $\Delta\nu_{\text{ind}}$  (inner right scale), and transmission peak of the transparency window  $T_{\text{ind}}$  (outer right scale), respectively. The solid, dashed, and dotted curves are the theoretical calculations, where  $x_1 = 0.999820$ ,  $y_1 = 0.999899$ , and  $x_2 = 0.999975$ .

$$\begin{aligned} A &= (1 - \gamma_1)^{1/2}[A_0 \cos(\kappa_1) - iB_0 \sin(\kappa_1)], \\ B &= (1 - \gamma_1)^{1/2}[-iA_0 \sin(\kappa_1) + B_0 \cos(\kappa_1)], \\ B_2 &= (1 - \gamma_2)^{1/2}[B_1 \cos(\kappa_2) - iC_0 \sin(\kappa_2)], \\ C &= (1 - \gamma_2)^{1/2}[-iB_1 \sin(\kappa_2) + C_0 \cos(\kappa_2)], \end{aligned} \quad (1)$$

where  $\gamma_1$  and  $\gamma_2$  are the insertion losses and  $\kappa_1$  and  $\kappa_2$  are the coupling strengths between the sphere and the fiber, and between the two spheres, respectively. The electrical fields are given as  $B_1 = B \exp[-\rho_1 L_1/4 - i\varphi_1(\nu)/2]$ ,  $B = B_2 \exp[-\rho_1 L_1/4 - i\varphi_1(\nu)/2]$ , and  $C_0 = C \exp[-\rho_2 L_2/2 - i\varphi_2(\nu)]$ , where  $\rho_1$  and  $\rho_2$  are the losses within  $S_1$  and  $S_2$ , respectively;  $L_1$  and  $L_2$  are the round-trip path lengths of the modes;  $\varphi_1(\nu) = 2\pi n_1 \nu L_1/c$ ,  $\varphi_2(\nu) = 2\pi n_2 \nu L_2/c$  are the phase shifts for a circulation within the sphere orbits;  $n_1 = n_2 = 1.458$  are the effective refractive indexes;  $c$  is the velocity of light in the vacuum. The output light electric field  $A(\nu)$  normalized by the incident light electric field  $A_0(\nu)$  is given as

$$\begin{aligned} \frac{A(\nu)}{A_0(\nu)} &= (1 - \gamma_1)^{1/2} \left[ \frac{y_1 - x_1 R_{S_2}(\nu) \exp(-i\varphi_1)}{1 - x_1 y_1 R_{S_2}(\nu) \exp(-i\varphi_1)} \right] \\ &= \sqrt{T(\nu)} \exp[-i\theta(\nu)], \end{aligned} \quad (2)$$

where

$$R_{S_2}(\nu) = (1 - \gamma_2)^{1/2} \left[ \frac{y_2 - x_2 \exp(-i\varphi_2)}{1 - x_2 y_2 \exp(-i\varphi_2)} \right],$$

$x_1 = (1 - \gamma_1)^{1/2} \exp(-\rho_1 L_1/2)$  and  $x_2 = (1 - \gamma_2)^{1/2} \exp(-\rho_2 L_2/2)$  are loss parameters, and  $y_1 = \cos(\kappa_1)$  and  $y_2 = \cos(\kappa_2)$  are coupling parameters, for  $S_1$  and  $S_2$ , respectively.  $T(\nu)$  and  $\theta(\nu)$  are the transmissivity and phase shift of the transmission light. The transmission spectrum and phase as a function of  $\nu$  depend sensitively on the coupling strength between the spheres and the losses. The typical trajectory of the transmitted field  $A(\nu)$  in a complex plane of  $\nu$  has a double-helical structure. The phase development as a function of laser frequency can be classified into three categories using real values  $z_i = \text{Re}[A(\nu_i)]$ , for  $i = 1, 2$ , and  $3$  at which the trajectory of the transmitted field on the complex plane crosses the real axis ( $\text{Im}[A(\nu_i)] = 0$ ). First, for the condition  $0 < z_1 = z_3 < z_2$  that appears typically when the  $S_1$  is undercoupled to the fiber,  $S_2$  modulates the loss and phase of the original  $S_1$  transmission, and a transparent window appears within the frequency region that is otherwise opaque. Under this regime, the frequency width of the induced transparency window is on the order of  $\Delta\nu \approx c\sqrt{2(1 - y_2)}/n_1 L_1 \pi$ , and the induced transmission peak increases as the coupling strength is increased and  $y_2$  is decreased, in good accordance with Fig. 2(b)–2(f). When the coupling strength increases further as  $x_2 > y_2$ , the transmission spectrum splits into two separate dips. This situation corresponds to a case of EIT where the Rabi frequency of the control laser field is larger than the excited state lifetime broadened linewidth. The solid curves in the left column of Figs. 2 and

3(a) show the calculated transmission spectra as a function of the frequency detuning. The parameters are given in the caption. We used the frequency difference between the two resonances,  $\Delta\nu_{12} = \nu_{S2} - \nu_{S1}$ , as a fitting parameter. Note that these calculations based on Eq. (2) corroborate the experimental observations well. We also calculated the transmission phase shift in the right column of Fig. 2 using the obtained loss and coupling parameters. For the frequency region of the induced transparency, the phase slope  $\partial\theta(\nu)/2\pi\partial\nu$  is positive and very steep linear normal dispersions appear. In this region, the pulses can propagate through the system with large positive delays without significant attenuation, amplification, or pulse deformation as experimentally demonstrated in Fig. 3(c). When the coupling strength increases, the slope of the phase at  $\nu_{S2}$  initially becomes steep in accordance with the increase of the height of the induced transmission peak. As the coupling strength increases further, and the width of the induced transparency window increases, the slope becomes gentle, in good accordance with Fig. 4. Fast light relevant to the anomalous dispersions in an undercoupled single microsphere-fiber taper system is also expected at both the lower and higher frequency sides of the transparent window. The solid curves in Figs. 3(b) and 4 are the calculated propagation delay time, where the concept of net group delay is applied and the spectral averaged  $\partial\theta(\nu)/2\pi\partial\nu$  is calculated [25]. We can see that directional coupling theory provides a quantitative explanation for the measured propagation delay times. In the present system, the minimum value of the bandwidth for the slow light  $\sim\Delta\nu$  is limited by the  $Q$  factor of the second sphere, while the maximum value is limited by the available maximum coupling strength. On the basis of a previous experiment [22], stronger coupling can also be viable when the two spheres are contacted closely, and we can expect much broader bandwidth over  $\Delta\nu \sim 100$  GHz.

Note that two other categories of transmission spectra appear depending on the coupling and loss parameters that can be physically be viable. When  $z_1 = z_3 < z_2 < 0$ , that appears when the  $S_1$  is overcoupled to the fiber ( $x_1 > y_1$ ), and  $S_2$  is weakly coupled to  $S_1$  [ $x_1 R_{S2}(0) > y_1$ ], the transmission spectrum shows induced absorption. In contrast to the induced transmission, the slope of the transmission phase becomes negative and fast light is expected. Finally, the third category is when  $z_1 = z_3 < 0 < z_2$ , that appears when the  $S_1$  is overcoupled to the fiber ( $x_1 > y_1$ ), and  $S_2$  is strongly coupled to  $S_1$  [ $x_1 R_{S2}(0) < y_1$ ], and the phase slope is positive over the resonance region.

In summary, we performed optical pulse propagation experiments and observed slow light using a system of coupled-resonator-induced transparency, which demonstrated the classical analogy of extremely slow light in EIT. Group index engineering in various photonic media and the realization of special resonance structures are challenging problems. The coupled-resonator-induced

transparency as well as EIT system may prove to be important because the propagation velocity can be controlled through the coupling strength. The reconfiguration rate in the present system may be limited by the bandwidth of the piezo-actuator, which may, however, be improved using electro-optical effect or nonlinear optical effect. Together with ultrahigh- $Q$  factors, this coupled microsphere system holds great promise for photonic applications and quantum-information technology.

- 
- [1] S. E. Harris, Phys. Today **50**, No. 7, 36 (1997).
  - [2] S. E. Harris, Phys. Rev. Lett. **62**, 1033 (1989).
  - [3] A. Imamoglu and S. E. Harris, Opt. Lett. **14**, 1344 (1989).
  - [4] L. V. Hau, S. E. Harris, Z. Dutton, and C. H. Behroozi, Nature (London) **397**, 594 (1999).
  - [5] C. Liu, Z. Dutton, C. H. Behroozi, and L. V. Hau, Nature (London) **409**, 490 (2001).
  - [6] D. F. Phillips, A. Fleischhauer, A. Mair, R. L. Walsworth, and M. D. Lukin, Phys. Rev. Lett. **86**, 783 (2001).
  - [7] J. J. Longdell, E. Fraval, M. J. Sellars, and N. B. Manson, Phys. Rev. Lett. **95**, 063601 (2005).
  - [8] K. J. Vahala, Nature (London) **424**, 839 (2003).
  - [9] Y. A. Vlasov, M. O'Boyle, H. F. Hamann, and S. J. McNab, Nature (London) **438**, 65 (2005).
  - [10] J. K. S. Poon, L. Zhu, G. A. DeRose, and A. Yariv, Opt. Lett. **31**, 456 (2006).
  - [11] Y. Hara, T. Mukaiyama, K. Takeda, and M. Kuwata-Gonokami, Phys. Rev. Lett. **94**, 203905 (2005).
  - [12] Y. P. Rakovich, J. J. Boland, and J. F. Donegan, Opt. Lett. **30**, 2775 (2005).
  - [13] B. M. Möller, U. Woggon, M. V. Artemyev, and R. Wanne-macher, Phys. Rev. B **70**, 115323 (2004).
  - [14] Q. Xu, B. Schmidt, S. Pradhan, and M. Lipson, Nature (London) **435**, 325 (2005).
  - [15] A. Naweed, G. Farca, S. I. Shopova, and A. T. Rosenberger, Phys. Rev. A **71**, 043804 (2005).
  - [16] D. D. Smith, H. Chang, K. A. Fuller, A. T. Rosenberger, and R. W. Boyd, Phys. Rev. A **69**, 063804 (2004).
  - [17] Q. Xu *et al.*, Phys. Rev. Lett. **96**, 123901 (2006).
  - [18] M. F. Yanik, W. Suh, Z. Wang, and S. Fan, Phys. Rev. Lett. **93**, 233903 (2004).
  - [19] M. F. Yanik and S. Fan, Phys. Rev. Lett. **92**, 083901 (2004).
  - [20] A. A. Savchenkov, V. S. Ilchenko, A. B. Matsko, and L. Maleki, Phys. Rev. A **70**, 051804(R) (2004).
  - [21] J. R. Buck and H. J. Kimble, Phys. Rev. A **67**, 033806 (2003).
  - [22] K. Totsuka and M. Tomita, Phys. Rev. E **75**, 016610 (2007).
  - [23] K. Totsuka and M. Tomita, J. Opt. Soc. Am. B **23**, 2194 (2006).
  - [24] L. F. Stokes, M. Chodorow, and H. J. Shaw, Opt. Lett. **7**, 288 (1982).
  - [25] A. I. Talukder, T. Haruta, and M. Tomita, Phys. Rev. Lett. **94**, 223901 (2005); also A. I. Talukder, Y. Amagishi, and M. Tomita, Phys. Rev. Lett. **86**, 3546 (2001).